

Exact Verification of First-Order Methods via Mixed-Integer Linear Programming

Vinit Ranjan, Stefano Gualandi, Andrea Lodi, and Bartolomeo Stellato

December 17, 2024

Abstract

We present exact mixed-integer programming linear formulations for verifying the performance of first-order methods for parametric quadratic optimization. We formulate the verification problem as a mixed-integer linear program where the objective is to maximize the infinity norm of the fixed-point residual after a given number of iterations. Our approach captures a wide range of gradient, projection, proximal iterations through affine or piecewise affine constraints. We derive tight polyhedral convex hull formulations of the constraints representing the algorithm iterations. To improve the scalability, we develop a custom bound tightening technique combining interval propagation, operator theory, and optimization-based bound tightening. Numerical examples, including linear and quadratic programs from network optimization and sparse coding using Lasso, show that our method provides several orders of magnitude reductions in the worst-case fixed-point residuals, closely matching the true worst-case performance.

1 Introduction

Convex Quadratic Programming (QP) is a fundamental class of optimization problems in applied mathematics, operations research, engineering, and computer science [12] with several applications from finance [39, 11] and machine learning [19, 57, 14, 34], to signal processing [40, 17] and model predictive control [10]. A particularly important subclass of QP is Linear Programming (LP) [20], which is widely used in scheduling [31], network optimization [8], chip design [36], and resource allocation [9]. In many such applications, solving the optimization problem is part of a wider system, imposing strict computational requirements on the algorithm used. In particular, these algorithms consist of repeated iterations, generating a sequence of points that converge to an optimal solution, if the problem is solvable. Depending on the operational speed of each application, the time available to solve each optimization problem may vary from minutes to milliseconds, which, in turn, sets an exact limit on the number of allowed iterations. Therefore, to safely deploy optimization

algorithms, we must ensure that they *always converge* within the prescribed iteration limit, *i.e.*, in real-time.

First-order optimization algorithms have attracted an increasing interest over the last decade due of their low per-iteration cost and memory requirements, and their warm-start capabilities. These properties are particularly useful, on the one hand, in large-scale optimization problems arising in data-science and machine learning, and, on the other hand, in embedded optimization problems arising in engineering and optimal control. First-order methods date back to the 1950s and were first applied to QPs for the development of the Frank-Wolfe algorithm [24]. Recently, several general-purpose solvers based on first-order methods have appeared, including PDLP [2, 3] for LP, OSQP [52] and QPALM [32] for QP, and SCS [42, 43] and COSMO [25] for conic optimization. These methods feature several algorithmic enhancements that make them generally reliable, including acceleration [42], and restarts [2, 3], which guarantee worst-case linear convergence rates. However, their exact non-asymptotic empirical behavior for a fixed budget of iterations is not clearly understood. In particular, their practical convergence behavior can be very different, and sometimes significantly better, than the worst-case bounds that do not account for any application-specific problem structure and warm-starts used.

In this paper, we introduce an exact and scalable Mixed-Integer Linear Programming (MILP) formulation of the problem of analyzing the performance of first-order methods in LP and QP.

1.1 The problem

We are interested in solving QPs of the form

$$\begin{aligned} & \text{minimize} && (1/2)z^T Pz + q(x)^T z \\ & \text{subject to} && Az + r = b(x) \\ & && r \in C_1 \times C_2 \times \cdots \times C_L, \end{aligned} \tag{1}$$

with variables $z \in \mathbf{R}^n$ and $r \in \mathbf{R}^m$, and instance parameters $x \in X \subseteq \mathbf{R}^p$, where X is a polyhedron. The sets $C_i \subseteq \mathbf{R}^{n_i}$ come from a selected list: the zero set $\{0\}^{n_i}$ to model equality constraints, the nonnegative orthant $\mathbf{R}_+^{n_i}$ to model one-sided inequality constraints, and the box $[\ell, u] \subseteq \mathbf{R}^{n_i}$ to model double-sided inequality constraints. We denote the objective as $f(z, x) = (1/2)z^T Pz + q(x)^T z$ with positive semidefinite matrix $P \in \mathbf{S}_+^n$ and affine function $q(x) \in \mathbf{R}^n$. The constraints are defined by matrix $A \in \mathbf{R}^{m \times n}$, and affine function $b(x) \in \mathbf{R}^m$. If $P = 0$, problem (1) becomes an LP. We focus on settings where we solve several instances of problem (1) with varying instance parameters x . We assume problem (1) to be solvable for any $x \in X$ and we denote the optimal solutions as $z^*(x)$. Problems where $q(x)$ and $b(x)$ change arise in a wide range of settings, including sparse coding using Lasso [57] (x being the input signal), model predictive control [10] (x being the state of a linear dynamical system), and network flow problems [8, Ch. 1] (x being the node supplies). Our goal is to solve problem (1) using *first-order methods* of the form

$$s^{k+1} = T(s^k, x), \quad k = 0, 1, \dots, \tag{2}$$

where T is a *fixed-point operator* that maps the (primal-dual) iterate $s^k \in \mathbf{R}^d$ to $s^{k+1} \in \mathbf{R}^d$ depending on the instance parameter x . We assume the operator to be L -Lipschitz in its first argument with $L > 0$ and, therefore, single-valued [49, Sec. 2.1]. Operators of this form encode a wide range of algorithms, including gradient descent, proximal gradient descent, and operator splitting algorithms [49]. We denote the initial iterate set as the polyhedron $S \subset \mathbf{R}^d$. For cold-started algorithms, we have $S = \{0\}$. For a given x , *fixed-points* $s^* = T(s^*, x)$ correspond to the (primal-dual) optimal solutions of problem (1) (*i.e.*, we can compute z^* from s^*). We define the *fixed-point residual* at iterate s^k for parameter x as $T(s^k, x) - s^k$. As $k \rightarrow \infty$, the fixed-point residual converges to 0 for common cases of operators (*e.g.*, averaged or contractive [5, Cor. 5.8, Thm. 1.50], [49, Thm. 1]). Therefore, the fixed-point residual is an easily computable measure of suboptimality and infeasibility.

We are interested in numerically verifying that the worst-case magnitude fixed-point residual after K iterations, is less than an accepted tolerance $\epsilon > 0$. Specifically, we would like to verify the following condition:

$$\|T^K(s^0, x) - T^{K-1}(s^0, x)\|_\infty \leq \epsilon, \quad \forall x \in X, s^0 \in S, \quad (3)$$

where T^K is the K -times composition of T . Note that the ℓ_∞ -norm is a standard way to measure convergence and is commonly used in most general purpose solvers [43, 2, 52, 29]. Verifying condition (3) boils down to checking if the optimal value of the following optimization problem is less than ϵ ,

$$\begin{aligned} \delta_K = \quad & \text{maximize} && \|s^K - s^{K-1}\|_\infty && \text{(VP)} \\ & \text{subject to} && s^{k+1} = T(s^k, x), \quad k = 0, 1, \dots, K-1, \\ & && s^0 \in S, \quad x \in X, \end{aligned}$$

where the variables are the problem parameters x and the iterates s^0, \dots, s^K . In the rest of the paper we will describe scalable ways to formulate and solve this problem as a MILP. We refer to (VP) as the *verification problem*.

1.2 Related works

Performance estimation. The optimization community has recently devoted significant attention on computed assisted tools to analyze the worst-case finite step performance of first-order optimization algorithms. Notable examples include the performance estimation problem (PEP) [22, 56, 55] approach that formulates the worst-case analysis as a semidefinite program (SDP), and the integral quadratic constraints (IQCs) framework that models optimization algorithms as dynamical systems, analyzing their performance using control theory [37]. Interestingly, solutions to IQCs can be viewed as feasible solutions of a specific PEP formulation searching for optimal linear convergence rate using Lyapunov functions [54]. By defining the appropriate constraints (*i.e.*, interpolation conditions), the PEP framework can model complex methods, including operator splitting [48] and stochastic optimization algorithms [53]. Thanks to user-friendly toolboxes such as PEPit [27], PEP has promoted

numerous discoveries, including the design of optimal algorithms by constructing custom inequality constraints [45], or by formulating the design problem as bilevel optimization where PEP serves as the subproblem [21]. By implicitly representing iterates and subgradients through their inner products, PEP cannot exactly describe the geometric location of the iterates and, therefore, it cannot accurately represent warm-starts [47]. Furthermore, PEP can only model function values and squared ℓ_2 -norms of vectors in the objective and constraints. This is a limitation because most solvers define termination criteria using ℓ_∞ -norms to uniformly bound the magnitude of the suboptimality and infeasibility errors [43, 2, 52, 29]. In contrast, in this work we formulate problems that exactly encode ℓ_∞ -norms and warm-starts using MILP.

Neural network verification. Our approach closely connects with the neural network verification literature. The main goal in this area is to verify that, for every allowable input (*e.g.*, all permissible pixel perturbations of training images), the output of a trained neural network satisfies certain properties (*e.g.*, correctly classifies the images). This ensures that there are *no adversarial examples* that are misclassified. Similarly, in this paper, we verify that at a given iteration, for every allowable problem instance, the norm of the residual remains below a precision threshold, ϵ , guaranteeing that there are *no adversarial problem instances* that are not solved to the desired precision. The neural network verification problem is inherently challenging and nonconvex, and various approaches frame it as a MILP [23, 59, 15] by encoding ReLU activation functions with discrete variables. Lifted representations of these activation functions can yield tighter problem relaxations and have been shown to reduce solution times [1, 58, 60]. However, successfully verifying large, general neural network architectures requires specialized branch-and-bound algorithms [13, 51] featuring specialized bound tightening [33], GPU-based bound propagation [61] and custom cutting planes [62]. Despite recent progress, the complex structure of trained neural networks still makes it challenging to verify architectures with tens of layers. While also relying on MILP formulations, our work exploits the specific convergence behavior of first-order methods to verify algorithm performance over tens of iterations. In addition, we model nonconvex iteration functions (*e.g.*, soft thresholding).

1.3 Our contributions

In this paper, we introduce a new MILP framework to exactly verify the performance of first-order optimization algorithms for LPs and QPs.

- We formulate the performance verification problem as a MILP where the objective is to maximize the ℓ_∞ -norm of the convergence residual after a given number of iterations. We model commonly used gradient, projection, and proximal steps as either affine or piecewise affine constraints in the verification problem.
- We construct convex hull formulations of piecewise affine steps of the form of the soft-thresholding operator, the rectified linear unit, and the saturated linear unit, and show that the corresponding separation problems can be solved in polynomial time.

- We introduce various techniques to enhance the scalability of the MILP. Specifically, we develop a custom bound tightening technique combining interval propagation, convergence properties from operator theory, and optimization-based bound tightening. Furthermore, we devise a sequential technique to solve the verification problem by iteratively increasing the number of steps until we reach the desired number of iterations.
- We benchmark our method against state-of-the-art computer assisted performance estimation techniques (PEP), on LP instances in network optimization and QP instances in sparse coding using Lasso, obtaining multiple orders of magnitude reduction on worst-case norm of the fixed point residual.

2 Mixed-Integer Linear Programming formulation

The remainder of this paper focuses on modeling (VP) using MILP techniques. Since often algorithms involve multiple steps for each iteration, we use the following notation to represent each iteration k :

$$s^{k+1} = T(s^k, x) \iff \begin{aligned} v^1 &= \phi_1(s^k, x) \\ v^2 &= \phi_2(v^1, x) \\ &\vdots \\ s^{k+1} &= \phi_l(v^{l-1}, x), \end{aligned} \quad (4)$$

where ϕ_1, \dots, ϕ_l are the intermediate step mappings. In the intermediate steps, proximal algorithms rely on evaluating the proximal operators [44, 6]. The proximal operator of a function $g : \mathbf{R}^d \rightarrow \mathbf{R} \cup \{+\infty\}$ is defined as $\mathbf{prox}_g(v) = \operatorname{argmin}_y (g(y) + (1/2)\|y - v\|_2^2)$. Most intermediate steps arising in LP and QP can be computed as either *affine* or *piecewise affine* steps [44, Sec. 6], which we express as MILP constraints.

2.1 Objective formulation

To model the ℓ_∞ -norm in the objective of problem (VP), we define $\delta_K = \|s^K - s^{K-1}\|_\infty = \|t\|_\infty$, with $t = s^K - s^{K-1}$ being the residual at the last step. Using the lower bounds $\underline{s}^{K-1}, \underline{s}^K$ and the upper bounds, \bar{s}^{K-1} and \bar{s}^K , of the last two iterates s^{K-1} and s^K , we can derive the lower and upper bounds on the residual t as $\underline{t} = \underline{s}^K - \bar{s}^{K-1}$ and $\bar{t} = \bar{s}^K - \underline{s}^{K-1}$. Then, by writing t as the difference of two nonnegative variables t^+ and t^- , *i.e.*, $t = t^+ - t^-$, we can represent the absolute value of its components as $t^+ + t^-$ and write δ_K as the following constraints

$$\begin{aligned} t &= t^+ - t^-, \quad t^+ \leq \bar{t} \odot w, \quad t^- \leq -\underline{t} \odot (\mathbf{1} - w) \\ t^+ + t^- &\leq \delta_K \leq t^+ + t^- + \max\{\bar{t}, -\underline{t}\} \odot (\mathbf{1} - \gamma) \\ \mathbf{1}^T \gamma &= 1, \quad t^+ \geq 0, \quad t^- \geq 0, \end{aligned} \quad (5)$$

where \odot is the elementwise product. Here, we introduced variable $w \in \{0, 1\}^n$ to represent the absolute values of the components of t , and variable $\gamma \in \{0, 1\}^d$ to represent the maximum inside the ℓ_∞ -norm.

2.2 Affine steps

Consider affine steps of the following form:

$$\phi(v, x) = \{w \in \mathbf{R}^d \mid Mw = By, \quad y = (v, x)\}, \quad (6)$$

where $M \in \mathbf{R}^{d \times d}$ is an invertible matrix and $B \in \mathbf{R}^{d \times (p+d)}$. We directly express these iterations as linear equality constraints for the verification problem (VP).

2.2.1 Explicit steps

When $M = I$, affine steps represent explicit iterate computations.

Gradient step. A gradient step of size $\eta > 0$ for a quadratic function $f(v, x) = (1/2)v^T P v + x^T v$ can be written as

$$\phi(v, x) = \{w \in \mathbf{R}^d \mid w = v - \eta \nabla f(v, x) = (I - \eta P)v - \eta x\}, \quad (7)$$

where $\nabla f(v, x) = P v + x$ is the gradient with respect to the first argument of f . Therefore, it is an affine step with $M = I$ and $B = [I - \eta P \quad -\eta I]$.

Momentum step. For a momentum step [41][47, Sec. 2.2], an operator is applied to a linear combination of iterates at both iteration k and iteration $k - 1$. Let g denote the intermediate step variables that momentum is applied to, and $v = (g^k, g^{k-1})$ is the concatenation of intermediate step variables from iteration k and $k - 1$. Given $\beta^k > 0$, momentum updates are defined by:

$$\begin{aligned} \tilde{v} &= g^k + \beta^k (g^k - g^{k-1}) \\ w &= \tilde{v} - \nabla f(\tilde{v}, x), \end{aligned}$$

and so can be written in our framework via substitution as:

$$\phi(v, x) = \{w \in \mathbf{R}^d \mid w = (1 + \beta^k)(I - \eta P)g^k - \beta^k(I - \eta P)g^{k-1} - \eta x\}.$$

Therefore, it is an affine step with $M = I$ and $B = [(1 + \beta^k)(I - \eta P) \quad -\beta^k(I - \eta P) \quad -\eta I]$.

Shrinkage operator. The shrinkage operator represents the proximal operator of the squared ℓ_2 -norm function $f(v) = (1/2)\|v\|^2$ [44, Sec. 6.1.1]. In this case, given $\lambda > 0$, we have

$$\phi(v, x) = \mathbf{prox}_{\lambda f}(v) = \{w \in \mathbf{R}^d \mid w = (1 + \lambda)^{-1}v\},$$

which is an affine step with $M = I$ and $B = [(1 + \lambda)^{-1}I \quad 0]$.

Fixed-schedule, average-based restarts. Similar to the momentum steps, fixed-schedule restarts consider a history of H previous iterates, where H is a predefined lookback window [2, 3]. This scheme averages the previous H iterates so that $w = (1/H) \sum_{j=k-H+1}^k g^j$. So, by defining $v = (g^k, g^{k-1}, \dots, g^{k-H+1})$, the restart can be written as

$$\phi(v, x) = \{w \in \mathbf{R}^d \mid w = (1/H)(\mathbf{1}^T \otimes I)v\},$$

where \otimes represents the Kronecker product and so $\mathbf{1}^T \otimes I$ is the horizontal stack of H copies of the identity matrix. This is an affine step with $M = I$, and $B = (1/H)(\mathbf{1}^T \otimes I)$.

Halpern anchor. Halpern mechanisms are also known as *anchoring* based methods [30, 46]. The anchoring step computes a weighted average with the *initial* iterate s^0 . So, an anchored gradient step is, given $\beta^k \in (0, 1)$, written as

$$w = \beta^k(g^k - \eta \nabla f(g^k, x)) + (1 - \beta^k)s^0.$$

By substituting in the gradient step (7) and letting $v = (g^k, s^0)$, we can write

$$\phi(v, x) = \{w \in \mathbf{R}^d \mid w = \beta^k((I - \eta P)g^k - \eta x) + (1 - \beta^k)s^0\},$$

which is an affine step with $M = I$ and $B = [\beta^k(I - \eta P) \quad (1 - \beta^k)I \quad -\beta^k \eta I]$.

2.2.2 Implicit steps

When $M \neq I$, affine steps represent implicit iterate computations that require linear system solutions with left-hand side matrix M .

Proximal operator of a constrained quadratic function. The proximal operator with $\lambda > 0$ of a convex quadratic function subject to linear equality constraints defined by $A \in \mathbf{R}^{m \times d}$, $b \in \mathbf{R}^m$, is given by

$$\mathbf{prox}_{\lambda f(\cdot, x)}(v) = \underset{\{Az=b\}}{\operatorname{argmin}} \left\{ (1/2)z^T P z + x^T z + 1/(2\lambda) \|z - v\|^2 \right\}. \quad (8)$$

The solution of (8) can be encoded as a linear system of equations defined by the KKT optimality conditions [12, Sec. 10.1.1]. These include steps in common algorithms such as OSQP [52] and SCS [43, 42], and projections onto affine sets [44, Sec. 6.2]. By introducing dual variable $\nu \in \mathbf{R}^m$, and defining $y = (v, x, b)$, the KKT conditions corresponding to the **prox** can be written as

$$\phi(w, x) = \left\{ w \in \mathbf{R}^{d+m} \mid \begin{bmatrix} P + \lambda^{-1}I & A^T \\ A & 0 \end{bmatrix} \begin{bmatrix} w \\ \nu \end{bmatrix} = \begin{bmatrix} \lambda^{-1}I & -I & 0 \\ 0 & 0 & I \end{bmatrix} y \right\},$$

and therefore can be written as an affine step with the corresponding matrices.

Proximal operator of an unconstrained quadratic function. The proximal operator of a convex quadratic function is a special case of (8) without the affine constraints and dual variables. As such, the constraints simplify to [44, Sec. 6.1.1]

$$\phi(v, x) = \mathbf{prox}_{\lambda f(\cdot, x)}(v) = \{w \in \mathbf{R}^d \mid (P + \lambda^{-1}I)w = v - x\},$$

which corresponds to an affine step with $M = P + \lambda^{-1}I$ and $B = [I \ -I]$.

Projection onto an affine subspace. The orthogonal projection onto the affine subspace defined by $Az = b$ is also a special case of (8) with $P = 0$, $x = 0$. We assume that A is a wide matrix ($m < d$) with linearly independent rows. By rearranging the terms, this can also be written as an explicit affine step of the form

$$\phi(v, x) = \mathbf{prox}_{\lambda f(\cdot, x)}(v) = \{w \in \mathbf{R}^d \mid w = (I - A^\dagger A)v + A^\dagger b\},$$

where $A^\dagger = A^T(AA^T)^{-1}$ is the pseudoinverse of A . Thus it also corresponds to an affine step with $M = I$ and $B = [I - A^\dagger A \ A^\dagger]$.

2.3 Piecewise affine steps

We consider elementwise separable piecewise affine steps of the form

$$(\phi(v, x))_i = \begin{cases} a_1^T y & y \in V_1 \\ a_2^T y & y \in V_2 \\ \vdots \\ a_h^T y & y \in V_h \end{cases} \quad \text{with } y = (v, x) \in \mathbf{R}^{d+p}, \quad (9)$$

for $i = 1, \dots, d$, where $a_1, \dots, a_h \in \mathbf{R}^{d+p}$ and V_1, \dots, V_h are disjoint polyhedral regions partitioning \mathbf{R}^{d+p} . We assume these steps to be monotonically nondecreasing in $y = (v, x)$. To model the piecewise affine behavior over disjoint regions of (9), we introduce binary variables. We derive an exact formulation of the convex hull of the regions

$$\Phi = \{(y, w) \in [\underline{y}, \bar{y}] \times \mathbf{R} \mid w = (\phi(v, x))_i \text{ with } y = (v, x)\}, \quad (10)$$

where the bounds are $\underline{y} = (\underline{v}, \underline{x}) \leq \bar{y} = (\bar{v}, \bar{x})$, for three common steps, the *soft-thresholding*, the *rectified linear unit*, and the *saturated linear unit*.

Soft-thresholding. We consider the composition of an affine function and the *soft-thresholding* operator with the form

$$(\phi(v, x))_i = \mathcal{T}_\lambda(a^T y) = \begin{cases} a^T y - \lambda & a^T y > \lambda \\ 0 & |a^T y| \leq \lambda \\ a^T y + \lambda & a^T y < -\lambda \end{cases} \quad \text{with } y = (v, x), \quad (11)$$

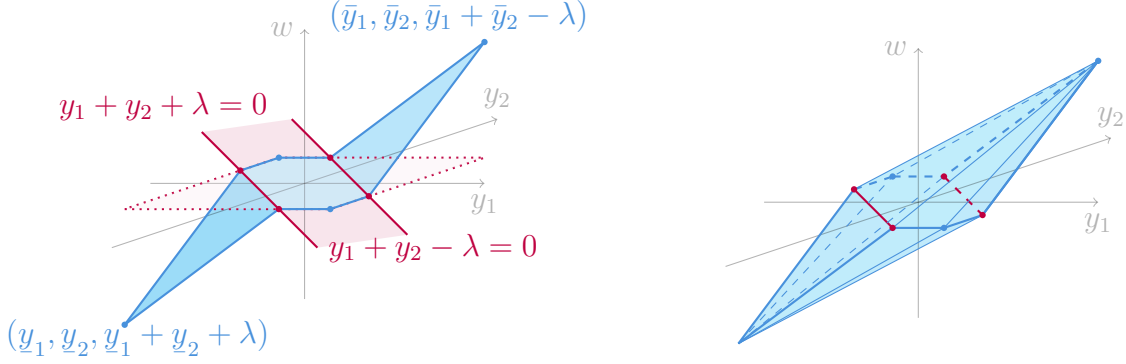


Figure 1: Left: Example of soft-thresholding $w = \mathcal{T}_\lambda(y_1 + y_2)$ with $\lambda = 0.5$ variable bounds $\underline{y}_1 \leq y_1 \leq \bar{y}_1$ and $\underline{y}_2 \leq y_2 \leq \bar{y}_2$; the two lines $y_1 + y_2 + \lambda = 0$ and $y_1 + y_2 - \lambda = 0$ delimit the area where $y = 0$. Right: the convex hull of $w = \phi_\lambda(y_1 + y_2)$ given by Theorem 2.1.

where \mathcal{T}_λ is the *soft-thresholding* operator with constant $\lambda > 0$, and $a \in \mathbf{R}^d$.

To formulate the step with big- M constraints, let

$$M^+ = \max_{y \in [\underline{y}, \bar{y}]} a^T y \quad \text{and} \quad M^- = \min_{y \in [\underline{y}, \bar{y}]} a^T y. \quad (12)$$

By introducing binary variables $\omega, \zeta \in \{0, 1\}$, we can formulate (11) as

$$\begin{aligned} a^T y - \lambda &\leq w \leq a^T y + \lambda \\ a^T y + \lambda - 2\lambda(1 - \zeta) &\leq w \leq a^T y - \lambda + 2\lambda(1 - \omega) \\ (M^- + \lambda)\zeta &\leq w \leq (M^+ - \lambda)\omega \\ \lambda + (M^- - \lambda)(1 - \omega) &\leq a^T y \leq \lambda + (M^+ - \lambda)\omega \\ -\lambda + (M^- + \lambda)\zeta &\leq a^T y \leq -\lambda + (M^+ + \lambda)(1 - \zeta). \end{aligned}$$

Note that, if $M^+ < \lambda$ or $M^- > -\lambda$, then we can prune at least one of the binary variables by setting it to zero.

In order to construct the convex hull of (11), we extend [58, Thm. 1] from the convex hull of the piecewise *maximum* of affine functions to the convex hull of nonconvex monotonically nondecreasing functions such as the soft-thresholding function. Figure 1 illustrates the operator $w = \mathcal{T}_\lambda(y_1 + y_2)$ with $\lambda = 0.5$ with its convex hull. Define vector $\ell^0 \in \mathbf{R}^d$ with entries $\ell_i^0 = \underline{y}_i$ if $a_i \geq 0$ and \bar{y}_i otherwise. Similarly, define vector $u^0 \in \mathbf{R}^d$ with entries $u_i^0 = \bar{y}_i$ if $a_i \geq 0$ and \underline{y}_i otherwise. Given $I \subseteq J = \{1, \dots, n\}$, define the lower bounds $\ell_I = \sum_{i \in I} a_i \ell_i^0 + \sum_{i \notin I} a_i u_i^0$ and the upper bounds $u_I = \sum_{i \in I} a_i u_i^0 + \sum_{i \notin I} a_i \ell_i^0$. We define the set of indices $\mathcal{I}^+ = \{(I, o) \in 2^J \times J \mid \ell_I \geq \lambda, \ell_{I \cup \{o\}} < \lambda, w_I \neq 0\}$ and $\mathcal{I}^- = \{(I, o) \in 2^J \times J \mid u_I \leq -\lambda, u_{I \cup \{o\}} > -\lambda, w_I \neq 0\}$, where w_I is the slicing of vector w over index set I . We can now obtain the convex hull of (11) with the following Theorem.

Theorem 2.1 (Convex hull of soft-thresholding operator). *Consider the region $\Phi =$*

$\{(y, w) \in [\underline{y}, \bar{y}] \times \mathbf{R} \mid w = \mathcal{T}_\lambda(a^T y)\}$. We can write its convex hull as

$$\mathbf{conv}(\Phi) = \left\{ (y, w) \in [\underline{y}, \bar{y}] \times \mathbf{R} \left| \begin{array}{l} w = a^T y - \lambda \quad \ell_J \geq 0 \\ w = a^T y + \lambda \quad u_J \leq 0 \\ w = 0 \quad -\lambda \leq \ell_J \leq u_J \leq \lambda \\ (y, w) \in Q \quad \text{otherwise} \end{array} \right. \right\}, \quad (13)$$

where

$$Q = \left\{ (y, w) \in \mathbf{R}^{d+p+1} \left| \begin{array}{l} a^T y - \lambda \leq w \leq a^T y + \lambda \\ \frac{\ell_J + \lambda}{\ell_J - \lambda} (a^T y - \lambda) \leq w \leq \frac{u_J - \lambda}{u_J + \lambda} (a^T y + \lambda) \\ w \leq \sum_{i \in I} a_i (y_i - \ell_i^0) + \frac{\ell_I - \lambda}{u_o^0 - \ell_o^0} (y_o - \ell_o^0), \quad \forall (I, o) \in \mathcal{I}^+ \\ w \geq \sum_{i \in I} a_i (y_i - u_i^0) + \frac{u_I + \lambda}{\ell_o^0 - u_o^0} (y_o - u_o^0), \quad \forall (I, o) \in \mathcal{I}^- \end{array} \right. \right\}.$$

Proof. Write the soft-thresholding operator as $w = \mathcal{T}_\lambda(a^T y) = w^+ - w^-$ where $w^+ = \mathbf{ReLU}(a^T y - \lambda)$ plus the bounds $-\lambda \leq y \leq \bar{y}$, and $w^- = \mathbf{ReLU}(-a^T y - \lambda)$ plus the bounds $\underline{y} \leq y \leq \lambda$. Using [58, Thm. 1], we can write the convex hull for the equalities defining w^+ and w^- and combine them. Using the fact that $w = w^+ - w^-$ we obtain the desired result. \square

Even though the constraints in Q define exponentially many inequalities, we can define an efficiently solvable separation problem: given a point (\hat{y}, \hat{w}) , verify that $(\hat{y}, \hat{w}) \in \mathbf{conv}(Q)$, otherwise return a violated inequality.

Proposition 2.1. *The separation problem for $\mathbf{conv}(\Phi)$ is solvable in $O(d + p)$ time.*

Proof. To check if $(\hat{y}, \hat{w}) \in \mathbf{conv}(Q)$, we first check if the point satisfies the first two sets of inequalities in $O(d + p)$ time. Note that (\hat{y}, \hat{w}) cannot violate the last two exponential sets of inequalities at the same time. Therefore, if $\hat{w} > 0$, we check if $\hat{w} \leq \min_{(I, o) \in \mathcal{I}^+} \sum_{i \in I} a_i (\hat{y}_i - \ell_i^0) + (\ell_I - \lambda) / (u_o^0 - \ell_o^0) (\hat{y}_o - \ell_o^0)$. Otherwise, if $\hat{w} < 0$, we check if $\hat{w} \geq \max_{(I, o) \in \mathcal{I}^-} \sum_{i \in I} a_i (\hat{y}_i - u_i^0) + (u_I + \lambda) / (\ell_o^0 - u_o^0) (\hat{y}_o - u_o^0)$. Both minimization and maximization problems can be theoretically solved in $O(n + p)$ time [58, Prop. 2]. If the conditions are satisfied, then $(\hat{y}, \hat{w}) \in \mathbf{conv}(Q)$. Otherwise, an optimal solution to these subproblems provides the most violated inequality. \square

Remark 2.1. We can also solve the separation problem in $O((d + p) \log(d + p))$ time by sorting the elements in nondecreasing order of $(\hat{y}_i - \ell_i^0) / (u_i^0 - \ell_i^0)$ (resp. $(\hat{y}_i - u_i^0) / (\ell_i^0 - u_i^0)$) and by iteratively including them to the set I until $\ell_I - \lambda < 0$ (resp. $u_I + \lambda > 0$). The last set I and index o that triggers the change of sign gives the most violated inequality for $\mathbf{conv}(Q)$ [58, Prop. 2].

We use these inequalities to tighten the root node relaxation by running the separation procedure for each component that corresponds to the output of a proximal step. We add the single most violated inequality, if any exist, to the MILP. These steps appear when

combining affine steps and proximal operators of nonsmooth functions. For example, the proximal gradient method with step size $\eta > 0$ applied to a Lasso [57] function of the form $f(z, x) = \|Dz - x\|_2 + \lambda\|z\|_1$ with $D \in \mathbf{R}^{p \times n}$ becomes the *iterative shrinkage thresholding algorithm* (ISTA) [6, Ch. 10] with iterations defined as $s^{k+1} = \mathcal{T}_{\lambda\eta}((I - \eta D^T D)s^k + \eta D^T x)$, where $\mathcal{T}_{\lambda\eta}$ applies the soft-thresholding operator elementwise. Therefore, with $v = s^k$, we can write ISTA iterations as

$$(\phi(v, x))_i = \mathcal{T}_{\lambda\eta}(((I - \eta D^T D)v + \eta D^T x)_i), \quad (14)$$

which corresponds to equation (11) with a being the i th row of $[I - \eta D^T D \quad \eta D^T]$.

Rectified linear unit. We consider the composition of an affine function and the *rectified linear unit* operator with the form

$$(\phi(v, x))_i = \mathbf{ReLU}(a^T y) = \max\{a^T y, 0\}. \quad (15)$$

Let us assume the constants from (12) to be $M^+ > 0$ and $M^- < 0$, otherwise ϕ is just a single linear equality. We can introduce a binary variable $\omega \in \{0, 1\}$, and write a formulation for (15) as

$$\begin{aligned} w &\geq 0, \quad w \geq a^T y \\ w &\leq a^T y - M^-(1 - \omega) \\ w &\leq M^+\omega. \end{aligned}$$

In this case, the convex hull of (10) can be directly described using [58, Thm. 1] which we restate here, for completeness.

Theorem 2.2 (Convex hull of rectified linear unit [58, Thm. 1]). *Consider the region $\Phi = \{(y, w) \in [\underline{y}, \bar{y}] \times \mathbf{R} \mid w = \mathbf{ReLU}(a^T y)\}$. Its convex hull is*

$$\mathbf{conv}(\Phi) = \left\{ (y, w) \in [\underline{y}, \bar{y}] \times \mathbf{R} \mid \begin{cases} w = a^T y & \ell_J \geq 0 \\ w = 0 & \ell_J < 0 \\ (y, w) \in Q & \text{otherwise} \end{cases} \right\}, \quad (16)$$

where

$$Q = \left\{ (y, w) \in \mathbf{R}^{d+p+1} \mid \begin{aligned} &w \geq a^T y, \quad y \geq 0 \\ &w \leq \sum_{i \in I} a_i (y_i - \ell_i^0) + \frac{\ell_I}{u_o^0 - \ell_o^0} (y_o - \ell_o^0), \quad \forall (I, o) \in \mathcal{I} \end{aligned} \right\}.$$

where ℓ_I, u_o^0 , and ℓ_o^0 are the same as in the soft-thresholding operator and the index set $\mathcal{I} = \{(I, o) \in 2^J \times J \mid \ell_I \geq 0, \ell_{I \cup \{o\}} < 0, w_I \neq 0\}$.

These steps appear when composing affine steps and projections onto the nonnegative orthant. For example, *projected gradient descent* with step size $\eta > 0$ applied to problem (1) with $q(x) = x$, $A = -I$, $b(x) = 0$, and $C = \mathbf{R}_+^n$, becomes $s^{k+1} = \Pi((I - \eta P)s^k - \eta x)$ where $\Pi = \mathbf{ReLU}$ clips the negative entries of its argument to 0. Therefore, with $v = s^k$, we can write the projected gradient descent iterations as

$$(\phi(v, x))_i = \mathbf{ReLU}(((I - \eta P)v - \eta x)_i),$$

which corresponds to equation (15) with a being the i th row of $[I - \eta P \quad -\eta I]$.

Saturated linear unit. Given two scalars $b, c \in \mathbf{R}$, we consider the composition of an affine function and the *saturated linear unit* with the form

$$(\phi(v, x))_i = \mathcal{S}_{[b, c]}(a^T y) = \begin{cases} b & a^T y < b \\ a^T y & b \leq a^T y \leq c \\ c & a^T y > c \end{cases} \quad \text{with } y = (v, x). \quad (17)$$

For the big- M formulation, we again introduce binary variables $\omega, \zeta \in \{0, 1\}$ arising from the three cases, and assume that the constants from (12) are $M^- < b$ and $M^+ > c$, otherwise we can prune some binary variables. We can write (17) as

$$\begin{aligned} b &\leq w \leq c \\ c - (c - b)(1 - \omega) &\leq w \leq b + (c - b)(1 - \zeta) \\ a^T y - (M^+ - M^-)\omega &\leq w \leq a^T y + (M^+ - M^-)\zeta \\ c + (M^- - c)(1 - \omega) &\leq a^T y \leq c + (M^+ - c)\omega \\ b + (M^- - b)\zeta &\leq a^T y \leq b + (M^+ - b)(1 - \zeta). \end{aligned}$$

Similarly to the soft-thresholding case, the saturated linear unit is a nonconvex monotonically nondecreasing function, so we again extend the results of [58, Thm. 1] and construct the convex hull of (17). Although we use a technique similar to that in the soft-thresholding case, we need to slightly redefine the variables from before, as shown in Theorem 2.3.

Theorem 2.3 (Convex hull of saturated linear unit). *For scalars $b, c \in \mathbf{R}$, and variable $y \in \mathbf{R}^d$, consider the region*

$$\Phi = \{(y, w) \in [y, \bar{y}] \times [b, c] \mid w = \mathcal{S}_{[b, c]}(a^T y)\}.$$

For $I \subseteq J = \{1, \dots, d\}$, let $\ell_I, u_I, \ell_i^0, u_i^0$ be defined in the same manner as for the soft-thresholding operator, but redefine the two index sets as $\mathcal{I}^+ = \{(I, o) \in 2^J \times J \mid \ell_I \geq b, \ell_{I \cup \{o\}} < b, w_I \neq 0\}$ and $\mathcal{I}^- = \{(I, o) \in 2^J \times J \mid u_I \leq c, u_{I \cup \{o\}} > c, w_I \neq 0\}$. We can express $\mathbf{conv}(\Phi)$ as

$$\mathbf{conv}(\Phi) = \left\{ (y, w) \in [y, \bar{y}] \times [b, c] \mid \begin{cases} w = b & u_J < b \\ w = c & \ell_J > c \\ w = a^T y & b \leq \ell_J \leq u_J \leq c \\ (y, w) \in Q & \text{otherwise} \end{cases} \right\},$$

where

$$Q = \left\{ (y, w) \in \mathbf{R}^{p+d+1} \mid \begin{aligned} &b \leq w \leq c \\ &\frac{b-c}{b-u_J}(a^T y - u_J) + c \leq w \leq \frac{c-b}{c-\ell_J}(a^T y - \ell_J) + b \\ &w \leq \sum_{i \in I} a_i(y_i - \ell_i^0) + \frac{\ell_J - b}{u_o^0 - \ell_o^0}(y_o - \ell_o^0) + b, \forall (I, o) \in \mathcal{I}^+ \\ &w \geq \sum_{i \in I} a_i(y_i - u_i^0) + \frac{u_J - c}{\ell_o^0 - u_o^0}(y_o - u_o^0) + c, \forall (I, o) \in \mathcal{I}^- \end{aligned} \right\}.$$

Proof. The operator (17) can be written as

$$\mathcal{S}_{[b,c]}(a^T y) = \min\{\max\{a^T y, b\}, c\}. \quad (18)$$

First consider the inner maximization, which can be rewritten as:

$$\max\{a^T y, b\} = \mathbf{ReLU}(a^T y - b) + b.$$

This allows us to apply Theorem 2.2, however we have to add the extra offset by b into $\mathbf{conv}(\Phi)$. The offset as well as the outer minimization means that we must remove the $w \geq a^T y$ constraint from the convex hull of the ReLU. For the rest of the hull, recognize that the order of the min and max in (18) can be swapped, so for the full description of the convex hull we must include the constraints from c as well. For these constraints, we use a similar rewriting:

$$\min\{a^T y, c\} = -\max\{-a^T y, -c\} = -\mathbf{ReLU}(-a^T y + c) + c.$$

Similar to the soft-thresholding case, we add the lower bound constraints on w but make sure to include the offset by c , which gives the complete result. \square

Remark 2.2. The separation procedure is similar to the one from the soft-thresholding case, with the only difference coming from the differing constants in the two index sets.

These steps appear when composing affine steps and projections onto boxes. For example, consider a QP of the form (1) with $q = x$, $A = -I$, $b(x) = 0$, and $C = [b, c]$ for $b, c \in \mathbf{R}^n$. Similarly to the ReLU case, a box-constrained QP of this form can be solved again with projected gradient descent with step size $\eta > 0$ with iterations $s^{k+1} = \mathcal{S}_{[b,c]}((I - \eta P)s^k - \eta x)$, where $\mathcal{S}_{[b,c]}$ applies the saturated linear unit elementwise. Therefore, with $v = s^k$, we can write projected gradient descent iterations as

$$(\phi(v, x))_i = \mathcal{S}_{[b_i, c_i]}(((I - \eta P)v - \eta x)_i) \quad (19)$$

which corresponds to equation (17) with a being the i th row of $[I - \eta P \quad -\eta I]$.

Example 2.1 (Vanilla MILP formulation). Consider the problem of recovering a sparse vector z^* from its noisy linear measurements $x = Dz^* + \varepsilon \in \mathbf{R}^p$, where $D \in \mathbf{R}^{p \times n}$ is the dictionary matrix and $\varepsilon \in \mathbf{R}^p$. A popular approach is to model this problem using Lasso [57] formulation with sparsity-inducing regularization parameter $\lambda > 0$

$$\text{minimize} \quad (1/2)\|Dz - x\|_2^2 + \lambda\|z\|_1. \quad (20)$$

The sparse coding problem (20) can be written as

$$\begin{aligned} &\text{minimize} \quad (1/2)z^T D^T D z - (x^T D^T)^T z + \lambda \mathbf{1}^T \mu \\ &\text{subject to} \quad -\mu \leq z \leq \mu, \end{aligned} \quad (21)$$

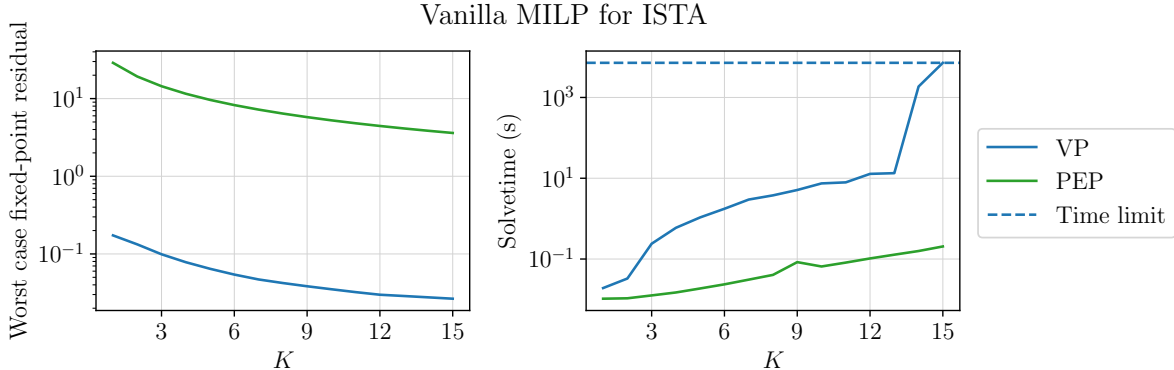


Figure 2: Left: Worst-case fixed-point residual norm for ISTA applied to (20) via VP and PEP. Right: Computation time to solve the respective optimization problems.

which corresponds to problem (1) with

$$P = \begin{bmatrix} D^T D & \\ & 0 \end{bmatrix} \in \mathbf{R}^{2n \times 2n}, \quad A = \begin{bmatrix} I & -I \\ -I & -I \end{bmatrix} \in \mathbf{R}^{2n \times 2n},$$

$q(x) = (-Dx, \lambda \mathbf{1}) \in \mathbf{R}^{2n}$, $b(x) = 0 \in \mathbf{R}^{2n}$, and $C = \mathbf{R}_+^{2n}$.

We choose $p = 15$, $n = 20$, $\lambda = 10^{-2}$, and, similarly to [18, Sec. 4.1], we sample the entries of D i.i.d. from the Gaussian distribution $\mathcal{N}(0, 1/m)$ with 20% nonzeros and normalize its columns. We generate 100 sparse vectors z^* with $z_i^* \sim \mathcal{N}(0, 1)$ with probability 0.1 and otherwise $z_i^* = 0$. We chose X to be the tightest hypercube containing all samples. We set $S = \{s^0\}$ where s^0 is the solution of the unregularized problem ($\lambda = 0$) for a random sample. We solve this problem with ISTA iterations of the form (14) with step size $\eta = 1/L$ where L is the largest eigenvalue of $D^T D$. Figure 2 shows that our formulation offers almost two orders of magnitude reduction in worst-case fixed-point residual, compared to PEP. However, without any scalability improvement (see next section), we are unable to solve such problems beyond $K = 15$ within the two hour time limit.

3 Scalability improvements

In this section, we describe the scalability improvements that allow us to solve (VP) for larger values of K . Our main idea is to solve (VP) *sequentially* from iteration 1 to K , by exploiting the optimal objective and the variable bounds obtained by solving previous problems. We also use the optimal solution at $K - 1$ to provide a feasible solution for (VP) at K .

3.1 Bound tightening

Interval propagation. Consider an affine step of the form (6). Using the factorization of M , we can convert the affine step to an explicit update $w = \tilde{B}y$ where $\tilde{B} = M^{-1}B$. Given lower and upper bounds y, \bar{y} , we can derive lower and upper bounds on w [28, Sec. 3] via

$w = (1/2)(\tilde{B}(\bar{y} + y) - |\tilde{B}|(\bar{y} - y))$, and $\bar{w} = (1/2)(\tilde{B}(\bar{y} + y) + |\tilde{B}|(\bar{y} - y))$, where $|\tilde{B}|$ is the elementwise absolute value of \tilde{B} . Consider now a piecewise affine step of the form (9). Since it is monotonically nondecreasing in its arguments, we can write bounds on w as $\underline{w} = \phi(\underline{v}, x)$ and $\bar{w} = \phi(\bar{v}, x)$. By chaining these bounds for all the steps in each iteration (4), we obtain interval propagation bounds $\underline{s}_{\text{ip}}^K \leq s^K \leq \bar{s}_{\text{ip}}^K$.

Operator theory based bounds. For a convergent operator T , the fixed-point residual is bounded by a decreasing sequence $\{\alpha_k\}_{k=1}^\infty$, *i.e.*, $\|s^k - s^{k-1}\|_\infty \leq \alpha_k$.

Proposition 3.1. *Let $\|s^k - s^{k-1}\|_\infty \leq \alpha_k$ and $\underline{s}^{k-1} \leq k^{K-1} \leq \bar{s}^{k-1}$. Then,*

$$\underline{s}^{k-1} - \alpha_k \leq s^k \leq \bar{s}^{k-1} + \alpha_k. \quad (22)$$

Proof. Since $\|s^k - s^{k-1}\|_\infty \leq \alpha_k$, we have $|s_i^k - s_i^{k-1}| \leq \alpha_k$. The absolute value implies $s_i^k - s_i^{k-1} \leq \alpha_k$ and $s_i^{k-1} - s_i^k \leq \alpha_k$. Replacing s_i^{k-1} by its upper and lower bounds, respectively, completes the proof. \square

In theoretical analysis of first-order methods, the bounding sequence α_k depends on the worst-case initial distance to optimality that we denote by $R = \sup_{x \in X, s^* \in S^*(x)} \|s^0 - S^*(x)\|_2$, where $S^*(x)$ is the set of (primal-dual) optimal solutions for instance x . Consider a β -contractive operator $T(\cdot, x)$ for any $x \in X$ with $\beta < 1$, which corresponds to a *linearly* convergent method. The fixed-point residual is bounded by $\alpha_k = 2\beta^{k-1}R$ [50, Sec. B.3]. Consider now an averaged operator $T(\cdot, x)$ for any $x \in X$, which corresponds to a *sublinearly* convergent method. In this case, the residual is bounded by $\alpha_k = (D/k^q)R$ for some $q > 0$ and D is a constant independent of K [49]. Using the fact that any vector ℓ_2 -norm is bounded above by its ℓ_1 -norm, we formulate a MILP analogous to that of problem (VP) using techniques from Section 2 to compute

$$R = \text{maximize } \|s^0 - s^*\|_1 \quad \text{subject to } s^* = T(s^*, x), \quad s^0 \in S, \quad x \in X, \quad (23)$$

over variables $s^* \in \mathbf{R}^d$ and $x \in \mathbf{R}^p$. These results give the operator theory based bounds $\underline{s}_{\text{ot}}^k = \underline{s}^{k-1} - \alpha_k \leq s^k \leq \bar{s}_{\text{ot}}^k = \bar{s}^{k-1} + \alpha_k$.

We apply both interval propagation techniques and operator theory bounds and use the tightest elementwise, *i.e.*, set the bounds as

$$\underline{s}^k = \max\{\underline{s}_{\text{ip}}^k, \underline{s}_{\text{ot}}^k\}, \quad \bar{s}^k = \min\{\bar{s}_{\text{ip}}^k, \bar{s}_{\text{ot}}^k\}. \quad (24)$$

Optimization-based bound tightening (OBBT). In practice, we tighten bounds \underline{s}^K and \bar{s}^K obtained in (24) with optimization-based bound tightening [26], by solving the following LP for each component of s^K

$$\begin{aligned} & \min(\max)\text{imize} && s_i^K \\ & \text{subject to} && (s^{k+1}, s^k) \in \mathbf{conv}(\{s^{k+1} = T(s^k, x)\}), \quad k = 0, \dots, K-1 \\ & && s^k \in [\underline{s}^k, \bar{s}^k], \quad k = 0, \dots, K. \end{aligned} \quad (25)$$

This procedure can be repeated until no more progress is made. In practice, we run 3 rounds of the optimization-based procedure before solving the MILP. The OBBT plays a crucial role in tightening the bounds of the y variables appearing in the definition of M^+ and M^- in (12). These tighter bounds lead to a tighter LP relaxation for each operator. Without the OBBT, we observe the big- M values are large and the MILPs do not scale to larger K .

3.2 Propagation between consecutive iterations

After solving the MILP (VP) at step K , we can use the resulting objective value t_K to post-process the bounds up to iteration K based on Proposition 3.2.

Proposition 3.2. *After solving (VP) until iteration K , obtaining objective values $\delta_1, \dots, \delta_K$, the following bounds hold on s^K :*

$$s_i^0 - \sum_{k=1}^K \delta_k \leq s_i^K \leq \bar{s}_i^0 + \sum_{k=1}^K \delta_k, \quad i = 1, \dots, d.$$

Proof. By definition of δ_K , $\|s^K - s^{K-1}\|_\infty \leq \delta_K$. Proposition 3.1 tells us that $s_i^{K-1} - \delta_K \leq s_i^K \leq s_i^{K-1} + \delta_K$. The proof is finished by induction on K and replacing s_i^0 by its bounds. \square

Therefore, as we solve (VP) for increasing values of K , we can postprocess and tighten the bounds for interval propagation and optimization-based bound tightening for later iterations.

4 Numerical experiments

We compare three baselines:

- **Sample maximum (SM).** We sample $N = 1000$ problems indexed by $\{x^i\}_{i=1}^N \in X$. For each sample, we then run the first-order method for $k = 1, \dots, K$ iterations and compute maximum ℓ_∞ -norm of the fixed-point residual. For all experiments, the sample maximum is a lower bound on the objective value of the VP.
- **Performance Estimation Problem (PEP).** We compute the worst-case objective from the PEP framework, which requires an upper bound R to the initial distance to optimality. We compute R as in equation (23), by using the squared ℓ_2 -norm in the objective obtaining a mixed-integer QP.
- **Verification Problem (VP).** We solve the MILP for the VP within a 5% optimality gap with a 2-hour time limit. We solve each MILP sequentially (see Section 3), and report the worst-case fixed-point residual norm.

We also compute the solution times for solving the VP and PEP. To observe the effects of (24), for each K we also count the fraction of iterate components where the operator theory bound is tighter than bound propagation. All examples are written in Python 3.12. We solve the MILPs using Gurobi 11.0 [29] with duality gap tolerance 5%. For PEP, we use

the PEPit toolbox [27], interfaced to MOSEK 10.2 [4]. All computations were run on the Princeton HPC Della Cluster with 28 CPU cores.

The code for all experiments can be found at

https://github.com/stellatogrp/mip_fom_experiments.

4.1 Sparse coding QP

We use the sparse coding settings given in Example 2.1. We analyze both the ISTA shown by (14) as well as the fast iterative shrinkage thresholding algorithm (FISTA) [7]. The FISTA iterations for problem (20) require an auxiliary sequence of iterates w^k with $w^0 = s^0$, and a scalar sequence $\beta_{k+1} = (1 + \sqrt{1 + 4\beta_k^2})/2$, with $\beta_0 = 1$ [7]. The iterations are given by

$$\begin{aligned} s^{k+1} &= \mathcal{T}_{\lambda\eta}((I - \eta D^T D)w^k + \eta D^T x) \\ w^{k+1} &= s^{k+1} + (\beta_k - 1)/\beta_{k+1}(s^{k+1} - s^k). \end{aligned} \tag{26}$$

Note that the β values are precomputed before forming the VP. Also, the worst-case fixed-point residual is only in terms of s^k and does not include the auxiliary sequence w^k .

We compare the ISTA vs FISTA for both strongly convex and nonstrongly convex examples. For the strongly convex example, we choose $p = 20$, $n = 15$ and for the nonstrongly convex example, we choose $p = 15$, $n = 20$. We use the same data generating procedure described in Example 2.1 and choose $\eta = 1/L$, where L is the maximum eigenvalue of $D^T D$. For the theory bounds, we apply results from [35, Thm. 2.2, Thm. 4.2].

Residual results are available in Figure 3, timing results are available in Figure 6 in Appendix A, and operator theory bound improvements are available in Appendix B. Our VP, in all cases, obtains two orders of magnitude reduction in the worst-case fixed-point residual norm over PEP. It is also more accurately able to capture the ripple behavior of FISTA, for which the residual norm does not monotonically decrease. FISTA takes longer to verify than ISTA due to the extra iterate sequence required for the algorithm, so we show the residuals up to $K = 30$ to be consistent across the algorithms. To show the effect of our scalability improvements, in Figure 4, we compare the solve times of the vanilla MILP formulation in Section 2 to the MILP with our improvements: those improvements allow the VP to scale up to $K = 40$.

4.2 Network optimization LP

We consider a minimum cost network flow problem [8] with varying node demands. Given a set of n_s supply nodes and n_d demand nodes, consider a bipartite graph on the node groups with capacitated directed edges from supply to demand nodes. Let A_s be the submatrix of rows corresponding to supply nodes and A_d be the submatrix of rows corresponding to demand nodes. For each edge i , let c_i be the flow capacity, μ_i be the cost of sending a unit of flow, and f_i be the variable representing the amount of flow sent. Lastly, let $b_s \geq 0$ be the vector of supply amounts available at each supply node and $x \leq 0$ be the amount of

Sparse coding

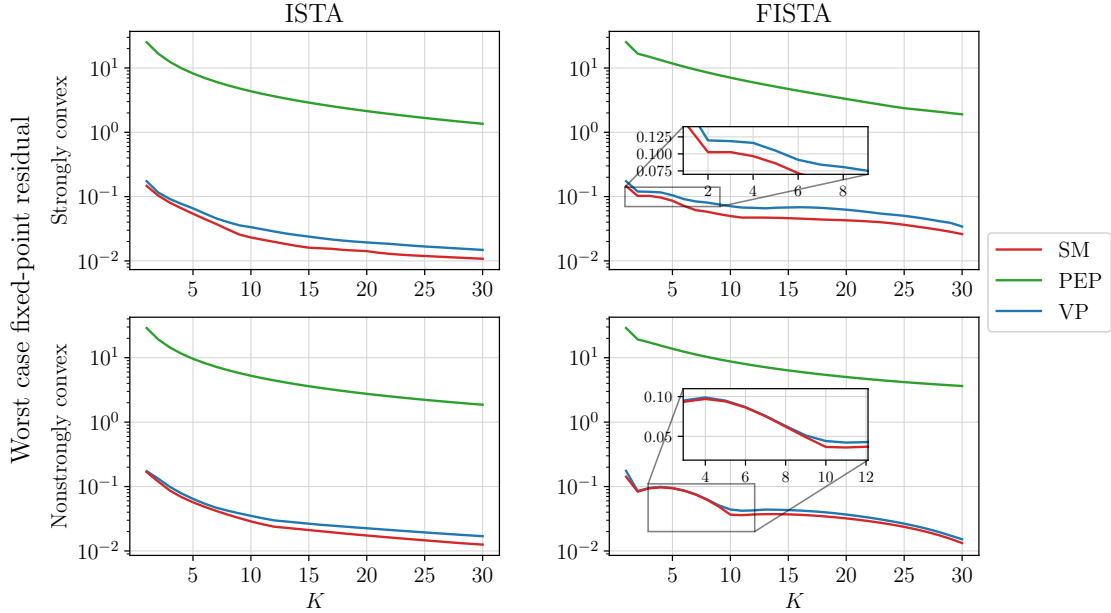


Figure 3: Worst-case fixed point residual norms for the ISTA (first column) and FISTA (second column) applied to (20). In the strongly convex case (first row, $p = 20, n = 15$), the acceleration results in a larger worst-case fixed-point residual up to $K = 30$ but we observe a reduction in the nonstrongly convex case (second row, $p = 15, n = 20$).

demand requested at each demand node. The minimum cost network flow problem can then be formulated as

$$\begin{aligned}
 & \text{minimize} && \mu^T f \\
 & \text{subject to} && A_s f \leq b_s \\
 & && A_d f = x, \\
 & && 0 \leq f \leq c,
 \end{aligned} \tag{27}$$

which corresponds to problem (1) with

$$P = 0 \in \mathbf{R}^{n_e \times n_e}, \quad A = \begin{bmatrix} -I \\ I \\ A_s \\ A_d \end{bmatrix} \in \mathbf{R}^{(n_s+n_d+2n_e) \times n_e},$$

$q(x) = \mu \in \mathbf{R}^{n_e}$, $b(x) = (0, c, b_s, x) \in \mathbf{R}^{n_s+n_d+2n_e}$, and $C = \mathbf{R}_+^{n_s+2n_e} \times \{0\}^{n_d}$.

We generate a random bipartite graph on 10 supply nodes and 5 demand nodes by adding each edge with probability 0.5. After generating the random graph and forming the LP, we obtain $A \in \mathbf{R}^{m \times n}$ with $m = 37, n = 54$. For this experiment, we keep a fixed supply $b_s = 10$ for each node and a fixed capacity $h = 4$ for each edge, and we sample the costs from i.i.d. from a uniform distribution $c_i \sim \mathcal{U}[5, 10]$. We parameterize only the demand as a unit

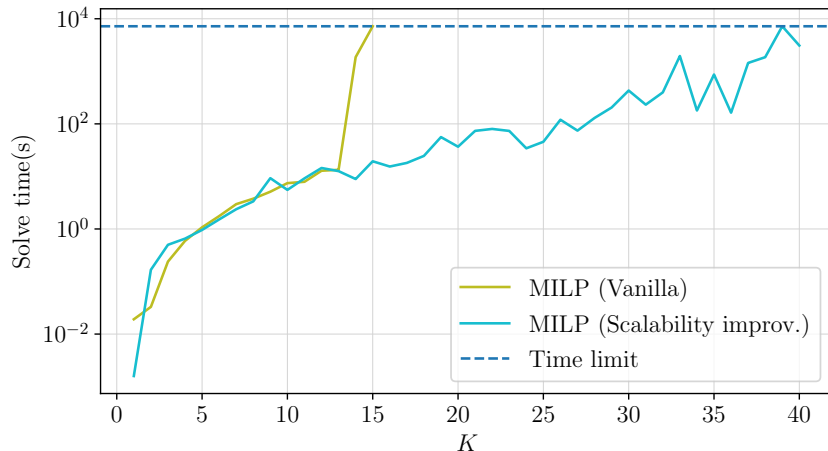


Figure 4: Solve times for the vanilla MILP defined in Section 2 vs. the MILP with our scalability improvements in Section 3 on the same nonstrongly convex instance.

hypercube $X = [-7, -5]^{n_d}$. For both algorithms, we choose the step size as $\eta = 0.5/\|A\|_2$. We choose s^0 to be the primal-dual solution to the problem instance where all demand nodes have maximum demand. If such an instance has a solution, then all instances in the family are feasible. For the theory bounds, we apply [38, Thm. 1].

We solve the problem using the primal-dual hybrid gradient (PDHG) algorithm [16] that operates on a primal and dual iterate $s^k = (z^k, w^k)$. We consider both the standard version of PDHG [16] with fixed step size $\eta > 0$ adapted to LPs [2, Eq. (1)], namely

$$\begin{aligned} w^{k+1} &= \max\{w^k - \eta(b(x) - Az^k), 0\} \\ z^{k+1} &= z^k - \eta(A^T(2w^{k+1} - w^k) + q(x)). \end{aligned} \quad (28)$$

We also consider a momentum accelerated version, with iterations given by

$$\begin{aligned} w^{k+1} &= \max\{w^k - \eta(b(x) - Az^k), 0\} \\ \tilde{w}^{k+1} &= w^{k+1} + k/(k+3)(w^{k+1} - w^k) \\ z^{k+1} &= z^k - \eta(A^T(2\tilde{w}^{k+1} - w^k) + q(x)), \end{aligned} \quad (29)$$

where we determine the momentum coefficients with Nesterov’s update rule [41]. Note that the algorithm is presented in this way for clarity, but in the verification problem, we substitute the \tilde{w}^{k+1} update into the z^{k+1} update. Residual results are available in Figure 5 and timing results are available in Figure 7 in Appendix A. In both cases, our VP is able to capture that the worst-case fixed-point residual norm is not monotonically decreasing. The momentum version is also able to obtain a smaller residual at around $K = 37$ after a large jump in the worst-case residual norm. Remarkably, the worst-case bound from PEP seems to diverge in the momentum case. This is consistent with prior results when problems lack strong convexity [37, Apx. B]. Instead, our approach is able to show convergence for this LP family up to $K = 50$.

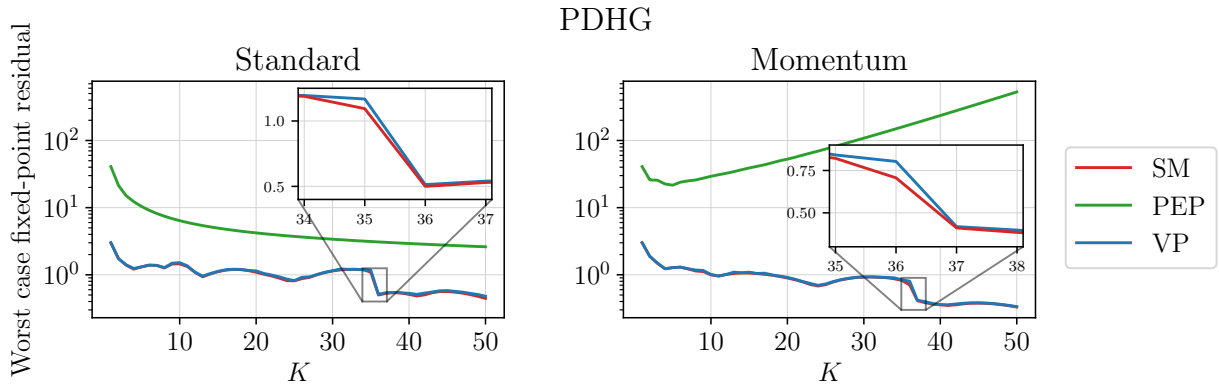


Figure 5: Worst-case fixed-point residual norms for the standard PDHG algorithm (left) and the version with momentum (right). Both algorithms show a rippling behavior and the momentum algorithm obtains a lower residual after a large step-like decrease.

Acknowledgements

Vinit Ranjan and Bartolomeo Stellato are supported by the NSF CAREER Award ECCS-2239771. The authors are pleased to acknowledge that the work reported on in this paper was substantially performed using the Princeton Research Computing resources at Princeton University which is consortium of groups led by the Princeton Institute for Computational Science and Engineering (PICSciE) and Research Computing.

Stefano Gualandi acknowledges the contribution of the National Recovery and Resilience Plan, Mission 4 Component 2 - Investment 1.4 - NATIONAL CENTER FOR HPC, BIG DATA AND QUANTUM COMPUTING (project code: CN_00000013) - funded by the European Union - NextGenerationEU.

References

- [1] R. Anderson, J. Huchette, W. Ma, C. Tjandraatmadja, and J. P. Vielma. Strong mixed-integer programming formulations for trained neural networks. *Mathematical Programming*, 183(1):3–39, 2020.
- [2] D. Applegate, M. Diaz, O. Hinder, H. Lu, M. Lubin, B. O’ Donoghue, and W. Schudy. Practical Large-Scale Linear Programming using Primal-Dual Hybrid Gradient. In *Advances in Neural Information Processing Systems*, volume 34, pages 20243–20257. Curran Associates, Inc., 2021.
- [3] D. Applegate, O. Hinder, H. Lu, and M. Lubin. Faster first-order primal-dual methods for linear programming using restarts and sharpness. *Mathematical Programming*, 201(1):133–184, 2023.
- [4] M. Aps. The MOSEK optimization software., 2024.

- [5] H. H. Bauschke and P. L. Combettes. *Convex Analysis and Monotone Operator Theory in Hilbert Spaces*. CMS Books in Mathematics. Springer International Publishing, Cham, 2017.
- [6] A. Beck. *First-Order Methods in Optimization*. Society for Industrial and Applied Mathematics, Philadelphia, PA, 2017.
- [7] A. Beck and M. Teboulle. A Fast Iterative Shrinkage-Thresholding Algorithm for Linear Inverse Problems. *SIAM Journal on Imaging Sciences*, 2(1):183–202, Jan. 2009.
- [8] D. P. Bertsekas. *Linear Network Optimization: Algorithms and Codes*. MIT press, 1991.
- [9] R. G. Bland. The Allocation of Resources by Linear Programming. *Scientific American*, 244(6):126–145, 1981.
- [10] F. Borrelli, Bemporad, Alberto, and Morari, Manfred. *Predictive Control for Linear and Hybrid Systems*. Cambridge University Press, 2017.
- [11] S. Boyd, E. Busseti, S. Diamond, R. N. Kahn, K. Koh, P. Nystrup, and J. Speth. Multi-Period Trading via Convex Optimization. *Foundations and Trends® in Optimization*, 3(1):1–76, 2017.
- [12] S. Boyd and L. Vandenberghe. *Convex Optimization*. Cambridge University Press, 2004.
- [13] R. R. Bunel, I. Turkaslan, P. Torr, P. Kohli, and P. K. Mudigonda. A Unified View of Piecewise Linear Neural Network Verification. In *Advances in Neural Information Processing Systems*, volume 31. Curran Associates, Inc., 2018.
- [14] E. Candès, M. Wakin, and S. Boyd. Enhancing sparsity by reweighted L1 minimization. *Journal of Fourier Analysis and Applications*, 14:877–905, Nov. 2007.
- [15] F. Ceccon, J. Jalving, J. Haddad, A. Thebelt, C. Tsay, C. D. Laird, and R. Misener. OMLT: Optimization & machine learning toolkit. *Journal of Machine Learning Research*, 23(349):1–8, 2022.
- [16] A. Chambolle and T. Pock. A First-Order Primal-Dual Algorithm for Convex Problems with Applications to Imaging. *Journal of Mathematical Imaging and Vision*, 40(1):120–145, May 2011.
- [17] S. S. Chen, D. L. Donoho, and M. A. Saunders. Atomic Decomposition by Basis Pursuit. *SIAM Review*, 43(1):129–159, 2001.
- [18] X. Chen, J. Liu, Z. Wang, and W. Yin. Theoretical Linear Convergence of Unfolded ISTA and its Practical Weights and Thresholds. In *Advances in Neural Information Processing Systems*, volume 31, pages 9079–9089. Curran Associates, Inc., 2018.
- [19] C. Cortes and V. Vapnik. Support-vector networks. *Machine Learning*, 20(3):273–297, 1995.

- [20] G. B. Dantzig. *Linear Programming and Extensions*. Princeton University Press, 1998.
- [21] S. Das Gupta, B. P. G. Van Parys, and E. K. Ryu. Branch-and-bound performance estimation programming: A unified methodology for constructing optimal optimization methods. *Mathematical Programming*, 204(1):567–639, 2024.
- [22] Y. Drori and M. Teboulle. Performance of first-order methods for smooth convex minimization: A novel approach. *Mathematical Programming*, 145(1):451–482, 2014.
- [23] M. Fischetti and J. Jo. Deep neural networks and mixed integer linear optimization. *Constraints*, 23(3):296–309, 2018.
- [24] M. Frank and P. Wolfe. An algorithm for quadratic programming. *Naval Research Logistics Quarterly*, 3(1-2):95–110, 1956.
- [25] M. Garstka, M. Cannon, and P. Goulart. COSMO: A Conic Operator Splitting Method for Convex Conic Problems. *Journal of Optimization Theory and Applications*, 190(3):779–810, 2021.
- [26] A. M. Gleixner, T. Berthold, B. Müller, and S. Weltge. Three enhancements for optimization-based bound tightening. *Journal of Global Optimization*, 67:731–757, 2017.
- [27] B. Goujaud, C. Mocer, F. Glineur, J. M. Hendrickx, A. B. Taylor, and A. Dieuleveut. PEPit: Computer-assisted worst-case analyses of first-order optimization methods in Python. *Mathematical Programming Computation*, 16(3):337–367, 2024.
- [28] S. Gowal, K. Dvijotham, R. Stanforth, R. Bunel, C. Qin, J. Uesato, R. Arandjelovic, T. A. Mann, and P. Kohli. Scalable Verified Training for Provably Robust Image Classification. In *2019 IEEE/CVF International Conference on Computer Vision (ICCV)*, pages 4841–4850, Seoul, Korea (South), Oct. 2019. IEEE.
- [29] Gurobi Optimization, LLC. Gurobi optimizer reference manual, 2024.
- [30] B. Halpern. Fixed points of nonexpanding maps. *Bulletin of the American Mathematical Society*, 73(6):957–961, 1967.
- [31] F. Hanssmann and S. W. Hess. A Linear Programming Approach to Production and Employment Scheduling. *Management Science*, MT-1(1):46–51, 1960.
- [32] B. Hermans, A. Themelis, and P. Patrinos. QPALM: A proximal augmented lagrangian method for nonconvex quadratic programs. *Mathematical Programming Computation*, 14(3):497–541, 2022.
- [33] C. Hojny, S. Zhang, J. S. Campos, and R. Misener. Verifying message-passing neural networks via topology-based bounds tightening, 2024.
- [34] P. Huber. Robust estimation of a location parameter. *The Annals of Mathematical Statistics*, 35(1):73–101, 1964.

- [35] D. Kim and J. A. Fessler. Another Look at the Fast Iterative Shrinkage/Thresholding Algorithm (FISTA). *SIAM Journal on Optimization*, 28(1):223–250, Jan. 2018.
- [36] J.-G. Kim and Y.-D. Kim. A linear programming-based algorithm for floorplanning in VLSI design. *IEEE Transactions on Computer-Aided Design of Integrated Circuits and Systems*, 22(5):584–592, 2003.
- [37] L. Lessard, B. Recht, and A. Packard. Analysis and Design of Optimization Algorithms via Integral Quadratic Constraints. *SIAM Journal on Optimization*, 26(1):57–95, 2016.
- [38] H. Lu and J. Yang. On the geometry and refined rate of primal–dual hybrid gradient for linear programming. *Mathematical Programming*, July 2024.
- [39] H. Markowitz. Portfolio selection. *The Journal of Finance*, 7(1):77–91, 1952.
- [40] J. Mattingley and S. Boyd. Real-time convex optimization in signal processing. *IEEE Signal Processing Magazine*, 27(3):50–61, 2010.
- [41] Y. Nesterov. A method for solving the convex programming problem with convergence rate $O(1/k^2)$. *Dokl akad nauk Sssr*, 269:543, 1983.
- [42] B. O’Donoghue. Operator splitting for a homogeneous embedding of the linear complementarity problem. *SIAM Journal on Optimization*, 31(3):1999–2023, 2021.
- [43] B. O’Donoghue, E. Chu, N. Parikh, and S. Boyd. Conic optimization via operator splitting and homogeneous self-dual embedding. *Journal of Optimization Theory and Applications*, 169(3):1042–1068, 2016.
- [44] N. Parikh and S. Boyd. Proximal Algorithms. *Foundations and Trends[®] in Optimization*, 1(3):127–239, 2014.
- [45] C. Park and E. K. Ryu. Optimal First-Order Algorithms as a Function of Inequalities. *Journal of Machine Learning Research*, 25(51):1–66, 2024.
- [46] J. Park and E. K. Ryu. Exact Optimal Accelerated Complexity for Fixed-Point Iterations. In *Proceedings of the 39th International Conference on Machine Learning*, volume 162 of *Proceedings of Machine Learning Research*, pages 17420–17457, June 2022.
- [47] V. Ranjan and B. Stellato. Verification of First-Order Methods for Parametric Quadratic Optimization, 2024.
- [48] E. K. Ryu, A. B. Taylor, C. Bergeling, and P. Giselsson. Operator Splitting Performance Estimation: Tight Contraction Factors and Optimal Parameter Selection. *SIAM Journal on Optimization*, 30(3):2251–2271, 2020.
- [49] E. K. Ryu and W. Yin. *Large-Scale Convex Optimization: Algorithms & Analyses via Monotone Operators*. Cambridge University Press, 1 edition, 2022.

- [50] R. Sambharya, G. Hall, B. Amos, and B. Stellato. Learning to Warm-Start Fixed-Point Optimization Algorithms. *Journal of Machine Learning Research*, 25(166):1–46, 2024.
- [51] Z. Shi, Q. Jin, Z. Kolter, S. Jana, C.-J. Hsieh, and H. Zhang. Neural Network Verification with Branch-and-Bound for General Nonlinearities, 2024.
- [52] B. Stellato, G. Banjac, P. Goulart, A. Bemporad, and S. Boyd. OSQP: An operator splitting solver for quadratic programs. *Mathematical Programming Computation*, 12(4):637–672, 2020.
- [53] A. Taylor and F. Bach. Stochastic first-order methods: Non-asymptotic and computer-aided analyses via potential functions. In *Proceedings of the Thirty-Second Conference on Learning Theory*, pages 2934–2992. PMLR, 2019.
- [54] A. Taylor, B. V. Scoy, and L. Lessard. Lyapunov Functions for First-Order Methods: Tight Automated Convergence Guarantees. In *Proceedings of the 35th International Conference on Machine Learning*, pages 4897–4906. PMLR, 2018.
- [55] A. B. Taylor, J. M. Hendrickx, and F. Glineur. Exact Worst-Case Performance of First-Order Methods for Composite Convex Optimization. *SIAM Journal on Optimization*, 27(3):1283–1313, 2017.
- [56] A. B. Taylor, J. M. Hendrickx, and F. Glineur. Smooth strongly convex interpolation and exact worst-case performance of first-order methods. *Mathematical Programming*, 161(1-2):307–345, 2017.
- [57] R. Tibshirani. Regression shrinkage and selection via the lasso. *Journal of the Royal Statistical Society: Series B*, 58(1):267–288, 1996.
- [58] C. Tjandraatmadja, R. Anderson, J. Huchette, W. Ma, K. Patel, and J. P. Vielma. The Convex Relaxation Barrier, Revisited: Tightened Single-Neuron Relaxations for Neural Network Verification. In *Advances in Neural Information Processing Systems*, volume 33, pages 21675–21686. Curran Associates, Inc., 2020.
- [59] V. Tjeng, K. Y. Xiao, and R. Tedrake. Evaluating robustness of neural networks with mixed integer programming. In *International Conference on Learning Representations*, 2019.
- [60] C. Tsay, J. Kronqvist, A. Thebelt, and R. Misener. Partition-Based Formulations for Mixed-Integer Optimization of Trained ReLU Neural Networks. In *Advances in Neural Information Processing Systems*, volume 34, pages 3068–3080. Curran Associates, Inc., 2021.
- [61] S. Wang, H. Zhang, K. Xu, X. Lin, S. Jana, C.-J. Hsieh, and J. Z. Kolter. Beta-CROWN: Efficient Bound Propagation with Per-neuron Split Constraints for Neural Network Robustness Verification. In *Advances in Neural Information Processing Systems*, 2021.

- [62] H. Zhang, S. Wang, K. Xu, L. Li, B. Li, S. Jana, C.-J. Hsieh, and J. Z. Kolter. General Cutting Planes for Bound-Propagation-Based Neural Network Verification. *Advances in Neural Information Processing Systems*, 35:1656–1670, 2022.

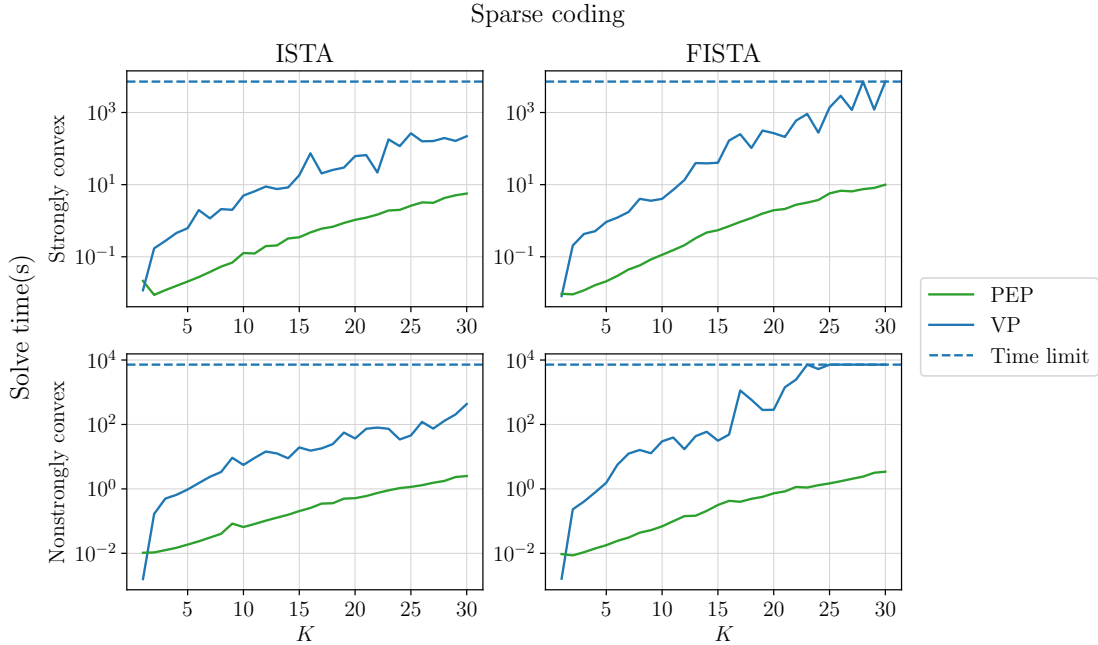


Figure 6: Solve time in seconds for all experiments shown in Figure 3. In both cases, FISTA takes longer to verify than ISTA as the extra iterate sequence from (26) causes the size of the MILP to increase.

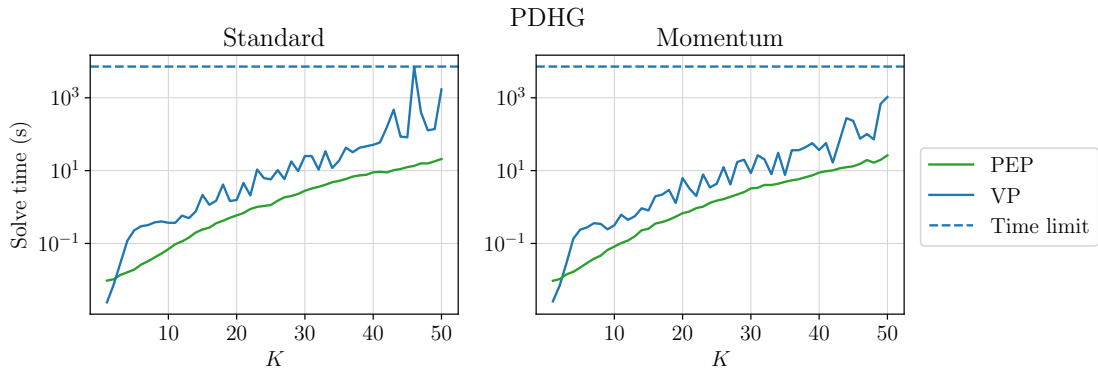


Figure 7: Solve time in seconds for all experiments shown in Figure 5. Both versions display similar overall growth in solve time.

A Full timing results

In this section we provide plots of all solve times in seconds for each experiment in Section 4. Figure 6 provides timing results for the experiments in Section 4.1 and Figure 7 provides timing results for the experiments in Section 4.2.

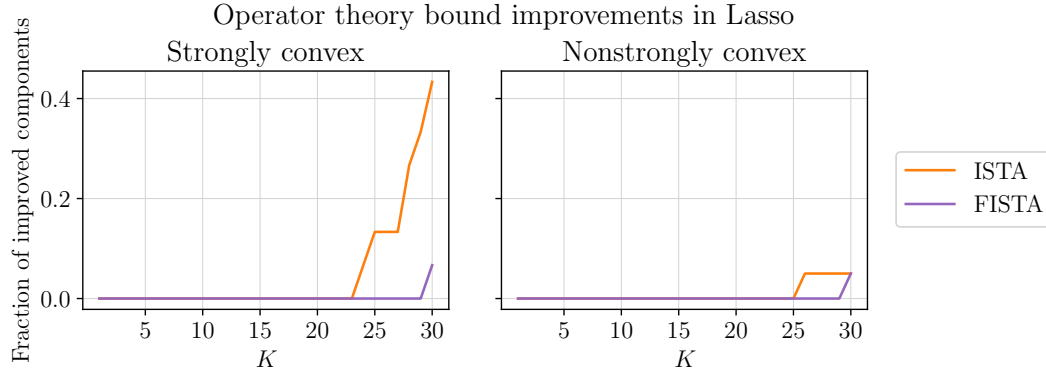


Figure 8: Fraction of iterate components in which the operator theory provides a tighter bound than interval propagation in the strongly convex (left) and nonstrongly convex (right) cases. The fractions correspond to the experiments in Figure 3. The operator theory bounds for ISTA are observed to be tighter for more indices than for FISTA, especially in the strongly convex case.

B Operator theory based improvements

Figure 8 shows the fraction of iterate indices where the operator theory based bound provides a tighter bound than interval propagation. Note that for the LP experiments with PDHG in Section 4.2, the operator theory bounds were never tighter than the interval propagation bounds, so we exclude plots for those algorithms.